

A reduced order model for Monte Carlo simulations of stochastic groundwater flow

Damiano Pasetto · Alberto Guadagnini · Mario Putti

2013/10/02

Keywords Groundwater hydrology · Randomly heterogeneous transmissivity · Monte Carlo simulations · Reduced Order Model · Greedy Algorithm

1 **Abstract** We explore the ability of the greedy algorithm to serve as an effective
2 tool for the construction of reduced order models for the solution of fully
3 saturated groundwater flow in the presence of randomly distributed transmissiv-
4 ities. The use of a reduced model is particularly appealing in the context of
5 numerical Monte Carlo (MC) simulations that are typically performed, e.g.,
6 within environmental risk assessment protocols. In this context, model order
7 reduction techniques enable one to construct a surrogate model to reduce the
8 computational burden associated with the solution of the partial differential
9 equation governing the evolution of the system. These techniques approximate
10 the model solution with a linear combination of spatially-distributed basis
11 functions calculated from a small set of full model simulations. The number
12 and the spatial behaviour of these basis functions determine the computational
13 efficiency of the reduced model and the accuracy of the approximated solu-

D. Pasetto

Institut National de la Recherche Scientifique,
Centre Eau Terre Environnement (INRS-ETE),
Université du Québec, G1K 9A9, Quebec City, Quebec, Canada
Now at Dipartimento di Matematica, University of Padova,
Via Trieste 63, 35121 Padova, Italy
E-mail: pasetto@math.unipd.it

A. Guadagnini

Dipartimento di Ingegneria Civile e Ambientale, Politecnico di Milano
Piazza L. Da Vinci 32, Milano, Italy
Department of Hydrology and Water Resources
University of Arizona, Tucson, Arizona 85721, USA
E-mail: alberto.guadagnini@polimi.it

M. Putti

Dipartimento di Matematica, University of Padova,
Via Trieste 63, 35121 Padova, Italy
E-mail: mario.putti@unipd.it

tion. The greedy algorithm provides a deterministic procedure to select the basis functions and build the reduced order model. Starting from a single basis function, the algorithm enriches the set of basis functions until the largest error between the full and the reduced model solutions is lower than a predefined tolerance. The comparison between the standard MC and the reduced order approach is performed through a two-dimensional steady-state groundwater flow scenario in the presence of a uniform (in the mean) hydraulic head gradient. The natural logarithm of the aquifer transmissivity is modeled as a second-order stationary Gaussian random field. The accuracy of the reduced basis model is assessed as a function of the correlation scale and variance of the log-transmissivity. We explore the performance of the reduced model in terms of the number of iterations of the greedy algorithm, and selected metrics quantifying the discrepancy between the sample distributions of hydraulic heads computed with the full and the reduced model. Our results show that the reduced model is accurate and is highly efficient in the presence of a small variance and/or a large correlation length of the log-transmissivity field. The flow scenarios associated with large variances and small correlation lengths require an increased number of basis functions to accurately describe the collection of the MC solutions, thus reducing significantly the computational advantages associated with the reduced model.

1 Introduction

Modeling groundwater flow in natural aquifers requires coping with spatial heterogeneity of hydraulic properties, e.g., hydraulic conductivity and/or transmissivity. A proper characterization of these parameters is the key to, e.g., optimize water management and accurately predict transport of contaminants. A deterministic approach to the solution of the flow problem is typically based on an estimation of the spatial distribution of the hydraulic parameter fields and the subsequent solution of the equations governing heads and fluxes. A stochastic approach (e.g., [1, 2]) describes parameters, such as aquifer transmissivity, as random fields with given probability distribution and aims at rendering the probability distribution of state variables, such as hydraulic heads and fluxes. A stochastic approach is appealing when sensitivity or uncertainty analyses of hydraulic head distributions are required in the presence of incomplete knowledge of the system parameters. It also enables one to embed methodologies such as Markov chain Monte Carlo (MC) and ensemble Data Assimilation for aquifer characterization under uncertainty (see e.g. [3, 4] and references therein).

Approaches that have been employed to solve the stochastic groundwater flow equation include moment differential equations (MDE) formulations, techniques based on partial differential equations satisfied by the probability density function (pdf) of the state variable of interest, and the numerical MC simulation framework. The idea underlying MDEs is the derivation of

56 deterministic equations satisfied by the statistical (ensemble) moments of hy-
57 draulic head from the constitutive groundwater equation and on the basis of
58 the knowledge of the (ensemble) moments of the system parameters, e.g., the
59 transmissivity field. The expected value and covariance of the hydraulic heads
60 are then numerically computed by way of recursive approximations of other-
61 wise nonlocal MDEs (see e.g. [5, 6]). The MDE approach has been recently em-
62 bedded within the context of Ensemble Kalman Filter based data assimilation
63 procedures of groundwater flow [7]. Current formulations of MDEs cannot be
64 easily extended to provide a complete characterization of the pdf of hydraulic
65 heads in the presence of randomly variable transmissivities, because of the
66 relatively complex formulation and prohibitive computational effort required
67 to compute statistical moments of order larger than two.

68 An alternative approach, which has been developed mainly in the context of
69 solute transport in randomly heterogeneous groundwater velocity fields (e.g.,
70 [8–11] and references therein), relies on the development of equations gov-
71 erning the space-time evolution of the pdf of solute concentrations. With the
72 exception of a few special cases, the solution of these equations typically en-
73 tails a series of approximations that are still limiting the direct application of
74 the approach to practical aquifer scale environmental problems.

75 MC-based methods rely on the generation of multiple independent and
76 identically-distributed realizations of the parameter fields driving groundwa-
77 ter flow. The corresponding solution of the flow equation yields a collection
78 of realizations of hydraulic heads from which ensemble statistics can be eval-
79 uated. Although the implementation of MC methods is straightforward also
80 in the presence of highly nonlinear models, the convergence of the empiri-
81 cal distribution to the underlying theoretical head probability distribution is
82 generally slow and may require a large number of computationally-expensive
83 solutions of the numerical model ([12] and references therein). For this rea-
84 son, a routine application of MC simulations to real field-scale aquifer systems
85 would significantly benefit from the development of a fast and accurate sur-
86rogate/reduced model for the computation of a large collection of hydraulic
87 head realizations [13].

88 Techniques based on the Polynomial Chaos Expansion (PCE) approxi-
89 mation may constitute a viable framework to obtain such surrogate system
90 models. PCE represents hydraulic head as a series of polynomials in terms of
91 a given set of random parameters. These polynomials are orthonormal to the
92 joint probability measure associated with the pdf of the uncertain system pa-
93 rameters ([14–17], and references therein). This expansion enables the efficient
94 computation of the moments of hydraulic head and, eventually, its complete
95 pdf. The spatially-distributed coefficients of the series are computed upon re-
96 lying on the solution of the flow equation according to the Galerkin projection
97 or the probabilistic collocation method (PCM) [18]. The number of elements to
98 retain in the series expansion and evaluations of the original groundwater flow
99 equation depends on the number of independent random parameters appear-
100 ing in the flow equation. For this reason the PCE is typically applied only in
101 the presence of a limited number of random parameters, an alternative being

102 the reliance on an approximation (e.g., truncated Karhunen-Loève expansion)
103 of the (spatially-distributed) stochastic parameters.

104 Surrogate models developed within the context of Galerkin projection meth-
105 ods are of critical interest for the reduction of the computational cost related
106 to the numerical evaluation of the collection of hydraulic head realizations. To
107 achieve accurate and sizeable reduction, these surrogate models are built by
108 projecting the original model equations onto a set of basis functions calculated
109 from a limited number of solutions of the complete model of the system. This is
110 typically termed *offline* phase, the *online* phase being the ensuing application
111 of the surrogate model to form the ensemble. The model reduction procedure
112 is computationally advantageous when the dimension of the reduced model,
113 i.e., the number of employed basis functions, is considerably smaller than that
114 of the original model. Proper orthogonal decomposition (POD) [19, 20] and
115 reduced basis (RB) [21, 22] are two model order reduction approaches that
116 compute spatially-distributed basis functions within an offline procedure based
117 on the snapshot technique. This technique relies on a collection of a certain
118 number of full system model solutions, i.e., the solutions of the original model
119 equations obtained for selected observation times and/or parameter values.
120 POD performs a singular value analysis on the set of the snapshots. The prin-
121 cipal components associated with the rightmost singular values constitute an
122 optimal set of basis functions for the reproduction of the snapshots, in the
123 sense that any other set of the same size reproduces the snapshots with a
124 larger error. Several examples of application of POD to reduce the computa-
125 tional burden associated with deterministic groundwater flow problems can be
126 found in the literature. Siade et al. [23] use POD in the context of inverse mod-
127 eling to accelerate estimation of aquifer transmissivities with quasilinearization
128 and quadratic programming. Kaleta et al. [24] and van Doren et al. [25] de-
129 velop a reduced order model for the solution of the flow equations for reservoir
130 simulation and the corresponding adjoint system. The principal component
131 analysis is critical to remove redundant information when a large number of
132 snapshots is available. The number of snapshots and principal components
133 that one should employ to obtain a reduced model with a desired accuracy on
134 the solution depends critically on the target model and cannot be quantified a
135 priori. For example, Pasetto et al. [13] show that the application of the POD
136 methodology in the presence of a stochastic and spatially-distributed recharge
137 (which constitutes an additive noise for the flow equation) is strongly affected
138 by the variance and correlation length of the recharge term.

139 The RB approach (see, e.g. [22]) relies on the computation of the full sys-
140 tem model solution only for those snapshots that maximize the amount of
141 information to be embedded in the reduced model. In this case, the orthonor-
142 malized snapshots are directly selected as basis functions, thus circumventing
143 the need for a principal component analysis. To determine the dimension of
144 the reduced model, a validation set of parameter values is first considered;
145 new snapshots are then sequentially added to the reduced model until the full
146 model solutions employed in the validation set are reproduced within a given
147 level of accuracy. The procedure for the selection of the snapshots is based on

148 the so-called greedy algorithm. Given a set of basis functions, a new snapshot
149 is computed by considering the parameter realization (selected amongst the
150 parameter realizations forming the validation set) that maximizes the discrep-
151 ancy between the full system model and the reduced model solutions. The
152 algorithm terminates when the maximum estimated error on each hydraulic
153 head solution of the validation set falls below a preselected tolerance. Since the
154 error between the reduced order and the full system model solutions cannot
155 be explicitly computed (because this requires the computationally expensive
156 full system model solution for all parameters in the validation set), the norm
157 of the residual is usually employed as a measure of the discrepancy between
158 the two solutions. Grepl and Patera [21] develop an *a posteriori* error bound
159 based on the computation of the residual to assess the accuracy of the reduced
160 model solution. This technique relies on an automatic procedure to establish
161 the basis functions that are required to achieve the reduction at a desired level
162 of accuracy. Pasetto et al. [26] demonstrate that the greedy algorithm is a
163 viable methodology to construct an accurate reduced model for the simulation
164 of groundwater flow in the presence of random transmissivity, when the latter
165 is described by a zonation approach. They show that the number of iterations
166 of the greedy algorithm, which coincides with the number of full system model
167 solutions, is determined by the error tolerance and the number of independent
168 random parameters (i.e., transmissivity zones) considered in the model.

169 Here, we study the implementation of the RB approach to construct a
170 reduced order model of steady-state groundwater flow driven by a randomly
171 distributed transmissivity field characterized by a log-normal probability den-
172 sity. The latter constitutes a multiplicative noise to the flow equation and still
173 represents a critical challenge in modern stochastic hydrogeology. We provide
174 a set of guidelines to establish the appropriate tolerance level to be set in the
175 greedy algorithm by considering a synthetic scenario representing a uniform
176 flow in the mean taking place within a two-dimensional bounded domain. The
177 convergence rate of the greedy algorithm is investigated as a function of the
178 correlation length and variance of the random transmissivity field. We explore
179 the relationship between the number of iterations of the greedy algorithm and
180 the reduced-model accuracy upon implementing the algorithm by considering
181 the explicit computation of the error on the basis of a large collection of MC
182 realizations. This allows circumventing inaccuracies related to the use of the
183 residual-based error estimations, which are only partially informative of the
184 head pdf stemming from MC simulations. The reliability of the heuristic crite-
185 ria underlying the application of the greedy algorithm is assessed in terms of
186 the maximum norm of the error between reduced order and full system model
187 results. Finally, we assess the accuracy of the reduced order model by compar-
188 ing the low order moments (ensemble mean and variance) and the empirical
189 probability distribution of nodal hydraulic heads resulting from a large set of
190 MC simulations performed with the full system model and the reduced order
191 model subject to different values of the error tolerance.

192 2 Problem Setting

193 We consider a fully saturated groundwater flow in a porous domain with ran-
194 dom hydraulic properties, described by the stochastic equation:

$$195 \quad \begin{cases} -\nabla \cdot (T(\mathbf{x}, \omega) \nabla h(\mathbf{x}, \omega)) = 0, & \mathbf{x} \in S \\ h(\mathbf{x}) = h_D(\mathbf{x}) & \mathbf{x} \in \partial S_D \subset \partial S \\ -T(\mathbf{x}, \omega) \nabla h(\mathbf{x}, \omega) = q_N(\mathbf{x}) & \mathbf{x} \in \partial S_N \subset \partial S \end{cases} \quad (1)$$

196 where \mathbf{x} is spatial-coordinate vector in the domain S ($S \subset \mathbb{R}^d$, $d = 1, 2$, or
197 3), ∂S is the boundary of the domain S , h is hydraulic head, ω is a random
198 sample in the space of outcomes Ω , and T is a randomly heterogeneous spa-
199 tial transmissivity field. The functions h_D and q_N are the hydraulic heads and
200 Darcy fluxes prescribed at the Dirichlet boundary ∂S_D and at the Neumann
201 boundary ∂S_N , respectively. We consider T as a stationary stochastic pro-
202 cess, characterized by a log-normal distribution, i.e., $Y = \log T$ is a Gaussian
203 random field, with uniform mean μ_Y and covariance function C_Y ,

$$204 \quad C_Y(r) = \sigma_Y^2 \rho_Y(r) \quad (2)$$

205 where r is separation distance (lag), and σ_Y^2 and $\rho_Y(r)$ are the variance and
206 the correlation function of Y , respectively.

207 The probability space is discretized by means of a number N_{ens} of MC sam-
208 ples. Let \mathcal{Y} be the set of the independent random realizations of Y employed in
209 the MC approach, $\mathcal{Y} = \{Y^{(1)}, \dots, Y^{(N_{ens})}\}$ and $\mathcal{T} = \{T^{(1)}, \dots, T^{(N_{ens})}\}$ the
210 corresponding transmissivities set. The numerical discretization of the flow
211 problem is obtained by means of the Galerkin finite element method with
212 piecewise linear elements on a triangular grid with n nodes. Solving Eq. 1 for
213 each element $T^{(i)} \in \mathcal{T}$ entails dealing with a high dimensional sparse linear
214 system

$$215 \quad \mathbf{A}^{(i)} \mathbf{h}^{(i)} = \mathbf{b} \quad (3)$$

216 where $\mathbf{A}^{(i)}$ is the stiffness matrix of dimension $n \times n$ associated with the
217 realization $T^{(i)}$, $\mathbf{h}^{(i)}$ is the vector of hydraulic heads at the grid nodes and
218 \mathbf{b} is the vector accounting for the boundary conditions. Hereafter we refer to
219 the solution of Eq. 3 as the full system model (FSM). Given the calculated
220 collection of MC realizations $\{h^{(1)}, \dots, h^{(N_{ens})}\}$, an ensemble moment μ of
221 hydraulic head at grid node x_j is approximated by its sample counterpart
222 μ^{FSM} :

$$223 \quad \mu(h(x_j)) = \int_{\mathbb{R}} \phi(h) p_h(h) dh \approx \mu^{FSM}(h_j) = \frac{1}{N_{ens}} \sum_{i=1}^{N_{ens}} \phi(h_j^{(i)}), \quad (4)$$

224 ϕ and p_h being an integrable function in probability space and the pdf of h at
225 node x_j , respectively.

226 3 Reduced Order Model and Greedy Algorithm

227 The reduced order model is constructed relying on a Galerkin projection tech-
 228 nique, which is at the basis of both the RB and POD methodologies. The vector
 229 of nodal hydraulic heads is approximated by the sum of a mean head field,
 230 $\mathbf{h}^{(0)}$ and a linear combination of N_{BF} spatially-distributed basis functions \mathbf{p}_j :

$$231 \quad \mathbf{h}^{(i)} \approx \tilde{\mathbf{h}}^{(i)} = \mathbf{h}^{(0)} + \sum_{j=1}^{N_{BF}} a_j^{(i)} \mathbf{p}_j = \mathbf{h}^{(0)} + \mathbf{P}\mathbf{a}^{(i)}. \quad (5)$$

232 Here, the vector of the coefficients $\mathbf{a}^{(i)} = \{a_1^{(i)}, \dots, a_{N_{BF}}^{(i)}\}$ depends on the ran-
 233 dom realization $T^{(i)}$, and \mathbf{P} is the matrix whose columns are the basis func-
 234 tions \mathbf{p}_j . The mean head field $\mathbf{h}^{(0)}$ may be approximated in different ways.
 235 For instance, one can employ the solution of Eq. 1 where T is replaced by the
 236 geometric mean of the transmissivity field (which is a relatively robust approx-
 237 imation of the mean head in the absence of forcing terms such as pumping).
 238 Alternatively, the solution of the approximated moment equations satisfied by
 239 the (ensemble) mean head can be used (see [5]). The coefficients $\mathbf{a}^{(i)}$ are com-
 240 puted in the reduced dimension, i.e., they are the solution of a linear system of
 241 dimension $N_{BF} \times N_{BF}$ (instead of being the solution of the $n \times n$ FEM system
 242 approximating the original groundwater flow model) obtained by projecting
 243 Eq. 3 onto the space generated by the N_{BF} basis functions \mathbf{p}_j , $j = 1, \dots, N_{BF}$.
 244 Hence, according to the Galerkin method, we substitute $\mathbf{h}^{(i)}$ with its approx-
 245 imation $\tilde{\mathbf{h}}^{(i)}$ in Eq. 3 and orthogonalize the residual with respect to the basis
 246 functions \mathbf{P} , obtaining the Reduced Order Monte Carlo model (ROMC):

$$247 \quad \tilde{\mathbf{A}}^{(i)} \mathbf{a}^{(i)} = \tilde{\mathbf{b}}^{(i)}, \quad (6)$$

248 where $\tilde{\mathbf{b}}^{(i)} = \mathbf{P}^T \mathbf{b} - \mathbf{P}^T \mathbf{A}^{(i)} \mathbf{h}^{(0)}$ and $\tilde{\mathbf{A}}^{(i)} = \mathbf{P}^T \mathbf{A}^{(i)} \mathbf{P}$ is a symmetric full
 249 matrix with dimension $N_{BF} \times N_{BF}$.

250 Solving Eq. 6 is computationally more advantageous than solving the FSM
 251 when the number of basis functions is significantly smaller than the num-
 252 ber of grid nodes, i.e. $N_{BF} \ll n$. This is balanced by the requirement that
 253 enough basis functions of sufficient quality should be employed to guarantee
 254 the accurate reproduction of the empirical pdf evaluated from the MC realiza-
 255 tions. Thus, the number of basis functions employed to achieve the reduction
 256 and their selection procedure characterize the reduced order model. Note that
 257 the reduction methodology can also be applied jointly with techniques that
 258 accelerate the convergence of the MC method, such as sparse grids, sparse ap-
 259 proximation, polynomial chaos expansion, latin hypercube, or multilevel MC
 260 (see e.g., [27]).

261 The POD and RB approaches employ basis functions extracted from a
 262 prescribed number of FSM solutions, which are termed snapshots.

263 In the POD method the snapshot technique [13] relies on collecting a num-
 264 ber N_{snap} of FSM solutions and performing a principal component analysis of

265 these snapshots. Then, the set of basis functions corresponds to the N_{BF} prin-
 266 cipal components associated with the rightmost singular values and provides
 267 the best approximation of the snapshots according to a predefined criterion.
 268 The number of snapshots, the criteria for their selection, and the number of
 269 principal components to use in the reduction process are (in principle) arbi-
 270 trary and strongly affect the quality of the reduction.

271 The RB method employs a different approach: the snapshots are computed
 272 using a greedy algorithm and are directly orthonormalized to form the set of
 273 basis functions used in the reduction. The greedy algorithm [28] is a deter-
 274 ministic methodology that enables one to obtain a set of suitable snapshots
 275 for the RB technique. The main advantage of this procedure with respect the
 276 POD method is that it requires only the collection of FSM solutions that are
 277 essential for the computation of the basis function set.

278 The greedy algorithm proceeds iteratively until some suitable metric quan-
 279 tifying the errors between the ROMC and FSM solutions is below a given
 280 tolerance τ . At each iteration the scheme augments the set of the basis func-
 281 tions with the realization associated with the largest error between the full and
 282 reduced model solutions. The idea underlying this choice is that the informa-
 283 tion content embedded in such a realization is not included in the current set
 284 of basis functions. Since the computation of the error is costly as it requires
 285 the knowledge of the FSM solution, the RB approach employs an *a posteriori*
 286 error estimation to assess the accuracy of the reduced model. If the error es-
 287 timation is larger than the tolerance τ , the reduced model is enriched with a
 288 new basis function, otherwise the algorithm terminates. The *a posteriori* error
 289 estimation is typically based on the computation of the residual associated
 290 with the reduced model solution to preserve the computational efficiency of
 291 the algorithm.

292 Here, we analyze the convergence properties of the greedy algorithm when
 293 applied to the MC solution of the stochastic PDE in Eq. 1. As noted in the
 294 introduction, a non accurate evaluation of the error estimate may lead to an
 295 inefficient reduced model. For this reason, our implementation of the greedy
 296 algorithm in the RB context relies on the exact computation of the errors in-
 297 stead of considering residual-based error estimates (as described, e.g., in [22]).
 298 At each k^{th} -iteration of the greedy algorithm we compute the ROMC solu-
 299 tions $\{\tilde{\mathbf{h}}_k^{(1)}, \dots, \tilde{\mathbf{h}}_k^{(N_{ens})}\}$ using $N_{BF} = k$ basis functions, $\mathbf{P}_k = [\mathbf{p}_1, \dots, \mathbf{p}_k]$.
 300 We consider the relative error measure defined as:

$$301 \quad \epsilon_k^{(i)} = \frac{\|\mathbf{h}^{(i)} - \tilde{\mathbf{h}}_k^{(i)}\|_\infty}{\|\mathbf{h}^{(i)}\|_\infty},$$

302 i.e., $\epsilon_k^{(i)}$ is the largest nodal error norm calculated between the i^{th} -solution
 303 of the FSM and the corresponding ROMC solution normalized by the largest
 304 head value of realization i . Let g_1, \dots, g_k be the indices of the head realiza-
 305 tions employed as snapshots in the k -th iteration of the greedy algorithm. If
 306 the largest value amongst the errors $\{\epsilon_k^{(1)}, \dots, \epsilon_k^{(N_{ens})}\}$ is smaller than the pre-
 307 defined tolerance τ , then the algorithm terminates. Otherwise, the set of basis

308 functions is enriched by employing the FSM solution that is associated with
 309 the largest value of the relative error $\epsilon_k^{(i)}$. In other words, at iteration $k + 1$
 310 we add the FSM realization characterized by the largest error norm, $\mathbf{h}^{(g_{k+1})}$
 311 to the set of previously calculated snapshots, where

$$312 \quad g_{k+1} = \arg \max_{1 \leq i \leq N_{ens}} \epsilon_k^{(i)}. \quad (7)$$

313 It follows that \mathbf{p}_{k+1} is the orthonormalization of $\mathbf{h}^{(0)} - \mathbf{h}^{(g_{k+1})}$ with respect
 314 to the set of the previously calculated basis functions, $\{\mathbf{p}_1, \dots, \mathbf{p}_k\}$. The ini-
 315 tialization of the greedy algorithm is performed by setting $k = 0$, $\tilde{\mathbf{h}}_0^{(i)} = \mathbf{h}^{(0)}$,
 316 and

$$317 \quad g_1 = \arg \max_{1 \leq i \leq N_{ens}} \epsilon_0^{(i)}, \quad \mathbf{p}_1 = \frac{\mathbf{h}^{(0)} - \mathbf{h}^{(g_1)}}{\|\mathbf{h}^{(0)} - \mathbf{h}^{(g_1)}\|_2}. \quad (8)$$

Algorithm 1 illustrates this methodology.

Algorithm 1 Greedy Algorithm

$k \leftarrow 0$

Compute $\mathbf{h}^{(0)}$

Compute $\{\epsilon_0^{(1)}, \dots, \epsilon_0^{(N_{ens})}\}$

while $\max_i \epsilon_k^{(i)} \geq \tau$ **do**

$k \leftarrow k + 1$

$g_k = \arg \max_i \epsilon_{k-1}^{(i)}$ (Eq. 7)

$\mathbf{p}_k = \mathbf{h}^{(0)} - \mathbf{h}^{(g_k)}$

 Orthonormalize \mathbf{p}_k with respect to $\{\mathbf{p}_1, \dots, \mathbf{p}_{k-1}\}$

$\mathbf{P}_k = [\mathbf{p}_1, \dots, \mathbf{p}_k]$

 Compute $\{\epsilon_k^{(1)}, \dots, \epsilon_k^{(N_{ens})}\}$

end while

318
 319 Several techniques are available in the literature to reduce the computa-
 320 tional cost associated with the greedy algorithm, as detailed in the following.
 321 Since the FSM solutions are typically not available, the norm of the residual
 322 term $\mathbf{r}_k^{(i)}$,

$$323 \quad \mathbf{r}_k^{(i)} = \mathbf{b} - \mathbf{A}^{(i)} \tilde{\mathbf{h}}_k^{(i)} \quad (9)$$

324 is usually employed for the evaluation of the error $\epsilon_k^{(i)}$ in Eq. 7 (see, e.g., [21,
 325 26]). The evaluation of the residual in Eq. 9 requires only the computation of
 326 the FSM solution of the realizations that maximize the norm of the residual.

327 Note that the norm of the residual can be computed in the reduced order space
 328 when $A^{(i)}$ is expressed as a linear combination of $N_m \ll n$ matrixes, i.e.

$$329 \quad \mathbf{A}^{(i)} = \sum_{j=1}^{N_m} c_j^{(i)} B^{(j)}, \quad (10)$$

330 where $B^{(1)}, \dots, B^{(N_m)}$ are parameter-independent matrixes of dimension $n \times n$
 331 while $c_1^{(i)}, \dots, c_{N_m}^{(i)}$ are coefficients depending on the random realization $T^{(i)}$.
 332 This is, e.g., the case when the random field T is approximated through the first
 333 N_m terms of the associated Karhunen-Loève expansion. Another procedure
 334 to accelerate the greedy algorithm is based on the computation of the basis
 335 functions relying either only on a subset of the original MC realizations or on
 336 particular samples of the random field [26].

337 Here, we analyze the way the empirical pdf obtained with the ROMC
 338 procedure depends on (i) the tolerance τ adopted in the greedy algorithm,
 339 (ii) the correlation length and (iii) variance of the log-transmissivity field. Our
 340 implementation of the greedy algorithm is based on the evaluation of the error
 341 on the FSM, without adding further approximations that can compromise the
 342 convergence of the greedy algorithm and the accuracy and efficiency of the
 343 resulting ROMC.

344 Given the approximated realizations $\{\tilde{\mathbf{h}}^{(1)}, \dots, \tilde{\mathbf{h}}^{(N_{ens})}\}$ obtained with Al-
 345 gorithm 1 at iteration k (the subscript is omitted for easier reading), the error
 346 between a given (ensemble) moment μ^{FSM} (Eq. 4) of the head at node x_j
 347 and its counterpart, μ^{ROMC} , calculated on the basis of the sample of ROMC
 348 realizations is given by:

$$349 \quad \begin{aligned} |\mu^{FSM}(h_j) - \mu^{ROMC}(\tilde{h}_j)| &\leq \sum_{i=1}^{N_{ens}} \frac{|\phi(h_j^{(i)}) - \phi(\tilde{h}_j^{(i)})|}{N_{ens}} \\ &= \sum_{i=1}^{N_{ens}} |\phi'(\xi_j^{(i)})| \frac{|h_j^{(i)} - \tilde{h}_j^{(i)}|}{N_{ens}} \leq C_j \sum_{i=1}^{N_{ens}} \frac{|\epsilon^{(i)}|}{N_{ens}} \leq C_j \tau, \end{aligned} \quad (11)$$

350 where $\xi_j^{(i)}$ is a point in the interval $[h_j^{(i)}, \tilde{h}_j^{(i)}]$ that satisfies the mean value
 351 theorem and $C_j = \max_i |\phi'(h_j^{(i)})| \|\mathbf{h}^{(i)}\|_\infty$. For example, one can note that
 352 $C_j = \max_i \|\mathbf{h}^{(i)}\|_\infty$ or $2 \max_i |h_j^{(i)}| \|\mathbf{h}^{(i)}\|_\infty$ for the first and second moment,
 353 respectively. Eq. 11 guarantees that the sample moments that are computed
 354 through the ROMC converge to the FSM moments when τ tends to zero. We
 355 also note that the error on the moments (Eq. 11) is bounded by the average
 356 nodal error. The latter can be, in turn, significantly smaller than the maxi-
 357 mum nodal error, and can be used as a termination condition for the greedy
 358 algorithm.

359 4 Numerical Example

360 We solve Eq. 1 in the two-dimensional domain S depicted in Fig. 1, which
 361 has a rectangular shape of length $L_x=18$ and $L_y=8$ units in the x and y

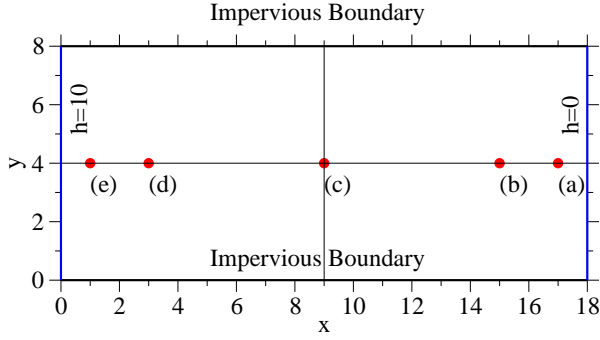


Fig. 1 Two-dimensional domain, S , employed in the numerical simulations. Location of control points considered in Fig. 7 is reported.

362 directions, respectively (here and in the following all quantities are given in
 363 consistent units). Prescribed heads of 10 and 0 are imposed at the left and
 364 right boundaries, respectively. Impervious boundary conditions are set at the
 365 top and bottom boundaries. The domain is discretized into 40×90 square
 366 cells, for a total of 3731 nodes.

367 The stationary log-transmissivity field, Y , is characterized by a normal
 368 probability distribution with $\mu_Y = 0$ and exponential isotropic covariance
 369 function,

$$370 \quad C_Y(r) = \sigma_Y^2 \exp\left(-\frac{r}{\lambda}\right), \quad (12)$$

371 where λ is the correlation length of Y . We analyze 24 test cases characterized
 372 by all the combinations of the following values of variance and relative domain
 373 size L_x/λ :

$$374 \quad \sigma_Y^2 = \{0.1, 0.2, 0.5, 1.0\}; \quad \frac{L_x}{\lambda} = \{9, 4.5, 3, 2.25, 1.8, 1.5\}. \quad (13)$$

375 For each of these cases we generate 10^4 independent MC realizations of the log-
 376 transmissivity field through the sequential Gaussian software HYDRO_GEN [29].
 377 We then solve the FSM equation (Eq. 3) for each transmissivity field and com-
 378 pute the empirical distribution of the hydraulic head at the grid nodes.

379 Algorithm 1 is employed for the construction of the reduced order model.
 380 We test four threshold values for the error tolerance, $\tau = \{8\%, 6\%, 4\%, 2\%\}$.
 381 For each of these tolerances we compute the collection of ROMC heads and
 382 compare their empirical pdf against the one obtained by way of the FSM
 383 realizations.

384 **5 Results and discussion**

385 5.1 Convergence of the greedy algorithm

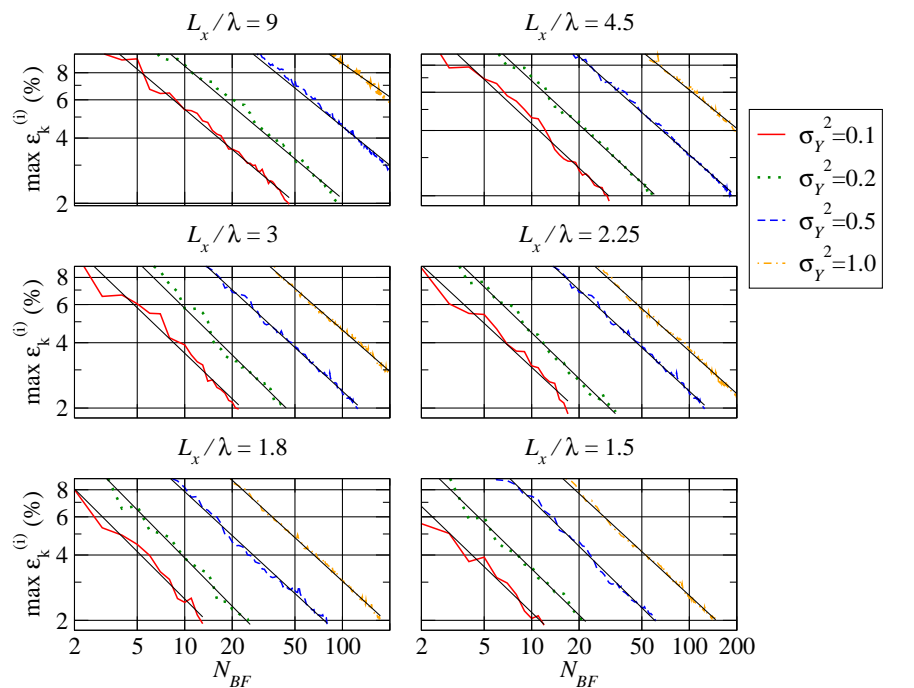


Fig. 2 Convergence of the maximum relative error $\epsilon_k^{(i)}$ with the number of basis functions N_{BF} employed in the reduced order model at each iteration of Algorithm 1. Results are illustrated for all 24 scenarios of log-transmissivity considered.

386 The number of iterations required to attain convergence of the greedy
 387 algorithm depends on the error tolerance τ and on the spatial variability of
 388 the random realizations of h . Realizations associated with large variability
 389 (both in space and in the ensemble sense) require an increased number of
 390 basis functions (i.e., of FSM solutions) to obtain approximation errors smaller
 391 than the tolerance τ .

392 Fig. 2 depicts (in log-log scale) the convergence of the maximum nodal error
 393 $\epsilon_k^{(i)}$ as a function of the number of iterations of the greedy algorithm for the 24
 394 test cases analyzed. For convenience, a maximum number of 200 iterations is
 395 set to terminate the algorithm. On one hand, we note that after 200 iterations
 396 the maximum error is still larger than the prescribed error tolerance when

| σ_Y^2 | m | | | | c | | | |
|----------------------|-------|-------|-------|-------|-------|-------|-------|-------|
| | 0.1 | 0.2 | 0.5 | 1.0 | 0.1 | 0.2 | 0.5 | 1.0 |
| $L_x/\lambda = 9$ | -0.61 | -0.61 | -0.59 | -0.51 | 0.223 | 0.351 | 0.685 | 0.935 |
| $L_x/\lambda = 4.5$ | -0.67 | -0.67 | -0.64 | -0.58 | 0.205 | 0.318 | 0.609 | 0.921 |
| $L_x/\lambda = 3$ | -0.69 | -0.71 | -0.66 | -0.63 | 0.177 | 0.299 | 0.519 | 0.854 |
| $L_x/\lambda = 2.25$ | -0.67 | -0.70 | -0.66 | -0.65 | 0.145 | 0.223 | 0.519 | 0.733 |
| $L_x/\lambda = 1.8$ | -0.72 | -0.73 | -0.67 | -0.66 | 0.133 | 0.211 | 0.367 | 0.646 |
| $L_x/\lambda = 1.5$ | -0.69 | -0.70 | -0.71 | -0.67 | 0.108 | 0.176 | 0.370 | 0.574 |

Table 1 Values of the order of convergence m and coefficient c of Eq. 14 for the 24 test cases analyzed.

397 $\tau = 2\%$ for the test cases associated with large variances and large relative
398 domain size (e.g., $L_x/\lambda=9, 4.5, 3, 2.25$, and $\sigma_Y^2=1.0$). On the other hand,
399 convergence is fast for settings with small relative domain size and variance
400 (e.g., $L_x/\lambda=1.8, 1.2$, and $\sigma_Y^2=0.1, 0.2$) and the imposed error tolerance is
401 obtained with less than 30 iterations. Fig. 2 also reports the regression lines
402 that approximate the convergence rate of the algorithm. These results reveal
403 that the convergence rate of the greedy algorithm is well approximated by a
404 power-law model of the kind:

$$405 \quad \max_i (\epsilon_k^{(i)}) \approx ck^m. \quad (14)$$

406 Table 1 summarizes the estimated values of c and m for the 24 test cases. The
407 order of convergence m slightly oscillates about a mean value of -0.66 and lies
408 within the range $[-0.73, -0.51]$. The coefficient c displays an approximately
409 linear dependence on the relative domain size L_x/λ and variance, its values
410 increasing from 0.108 in the case with $L_x/\lambda=1.5, \sigma_Y^2=0.1$ to 0.935 for $L_x/\lambda=9,$
411 $\sigma_Y^2=1.0$.

412 These results may be explained by the observation that large correlation
413 lengths of the Y field (i.e., low values of L_x/λ) are associated with relatively
414 smooth spatial variations of h . This implies that the ensemble variance of
415 hydraulic heads tends to decrease with decreasing L_x/λ for the flow condition
416 considered. As a consequence, only few basis functions are required to describe
417 the realizations of head, and the greedy algorithm converges more rapidly.
418 A corresponding argument explains the behavior observed for the settings
419 associated with low variance of Y .

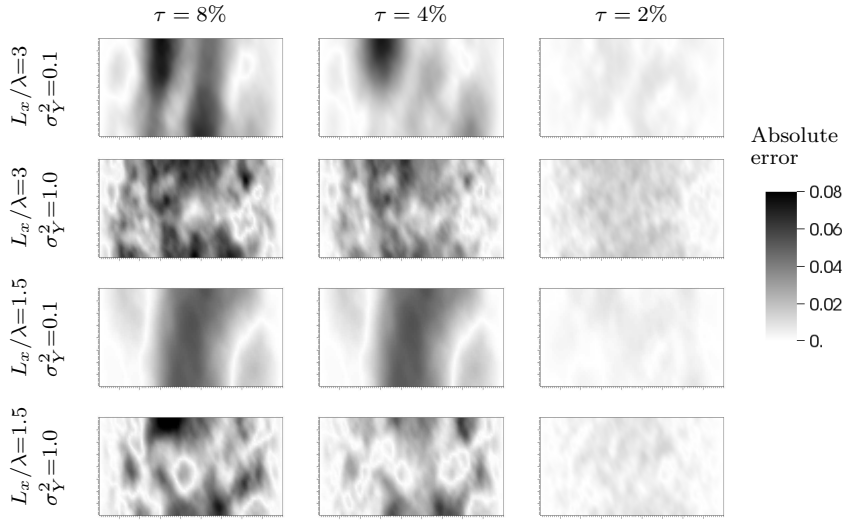


Fig. 3 Spatial distribution of the absolute error between the empirical variances of the hydraulic head realizations computed with the FSM and the ROMC. Results for four test cases (corresponding to all combinations of $L_x/\lambda=3, 1.5$ and $\sigma_Y^2=1.0, 0.1$) and three error tolerances $\tau=8\%, 4\%, 2\%$. are shown.

420 5.2 Estimation of head variance

421 Here, we analyze the accuracy of the ROMC procedure for the approximation
 422 of the empirical variance of hydraulic heads. Figs. 3 and 4, respectively, depict
 423 the spatial distribution of the absolute and relative errors between the empir-
 424 ical variances computed via the FSM and the ROMC. Results are illustrated
 425 for four selected test cases (corresponding to all combinations of $L_x/\lambda=3, 1.5$
 426 and $\sigma_Y^2=1.0, 0.1$) and three error tolerances $\tau=8\%, 4\%, 2\%$. In agreement
 427 with Eq. 11, the error on the variance decreases throughout the domain as τ
 428 decreases, its values always being of the same order of magnitude as those of
 429 τ (see Fig. 3). This in turn implies that Eq. 11 can be considered as a conser-
 430 vative upper bound on the error performed by the ROMC on the computation
 431 of the second moment.

432 Note that the magnitude of the absolute errors depicted in Fig. 3 does
 433 not display large variations for a given error tolerance. This implies that τ
 434 controls the accuracy of the reproduction of the collection of MC realizations
 435 and their statistics. This result is consistent with Eq. 11, where it is seen
 436 that the error is independent of the correlation length and variance of Y . The
 437 generality of this conclusion within the range of parameters tested is supported
 438 by Fig. 5, where the boxplots of the distribution of the spatial nodal errors

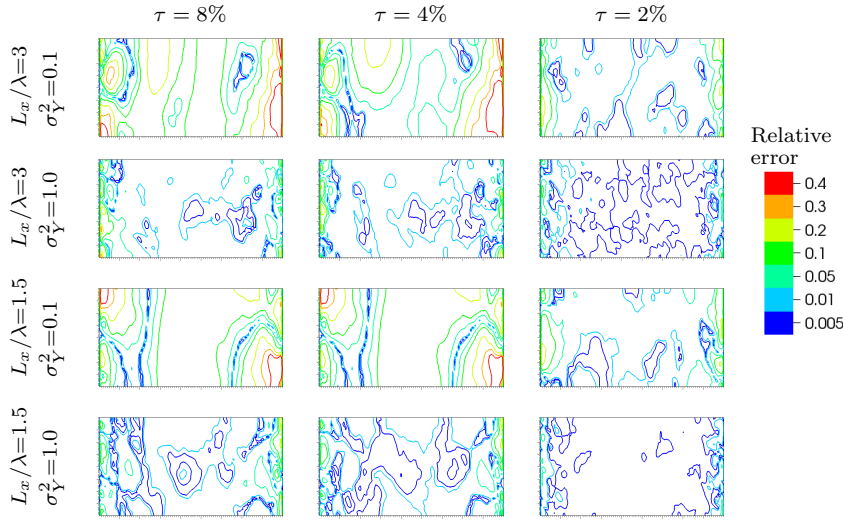


Fig. 4 Spatial distribution of the relative error between the empirical variances of the hydraulic head realizations computed with the FSM and the ROMC. Results for four test cases ($L_x/\lambda=3, 1.5$ and $\sigma_Y^2=1.0, 0.1$) and three error tolerances $\tau=8\%, 4\%, 2\%$. are shown.

439 on the head variance are shown for the complete set of test cases and the four
 440 error tolerances analyzed. Fig. 4 reveals that the largest relative nodal errors
 441 occur in the proximity of the Dirichlet boundary, i.e. where the head variance
 442 tends to vanish, while they are always smaller than the desired model accuracy
 443 at all other locations in the domain.

444 5.3 Empirical distributions of nodal heads

445 MC simulations are frequently employed (e.g., in environmental risk assess-
 446 ment protocols) to explore the behavior at the tails of the probability distri-
 447 bution. Here, we focus on the ability of the ROMC scheme to approximate the
 448 10^{th} - and 90^{th} -percentiles of nodal heads distributions, q_{10} and q_{90} , respec-
 449 tively defined as:

$$450 \quad P(h < q_{10}) = 10\% , \quad P(h < q_{90}) = 90\% \quad (15)$$

451 where P indicates probability. Figs. 6 and 7 report the relative errors on the
 452 q_{10} and q_{90} for hydraulic heads at nodes located along the central vertical
 453 cross-section of the domain, where head variances are highest. By way of il-
 454 lustration and consistent with Figs. 3 and 4, the results are presented for the
 455 test cases associated with all combinations of $L_x/\lambda=3, 1.5$ and $\sigma_Y^2=1.0, 0.1$.

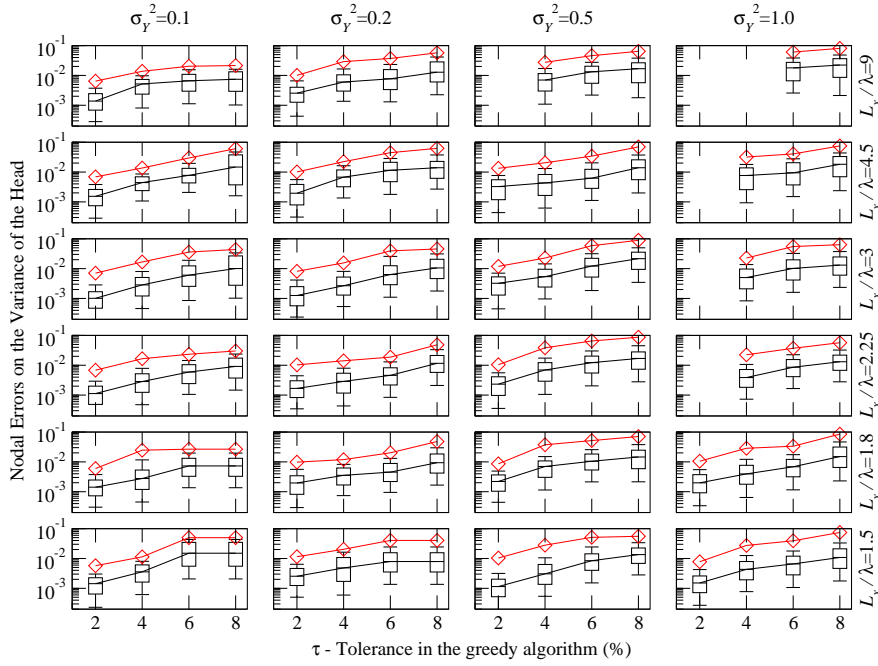


Fig. 5 Distribution of the nodal errors between the empirical hydraulic head variances computed with the FSM and the ROMC. Each boxplot depicts the 10th, 25th, 50th, 75th and 90th percentile of the error distributions. The red curves represent the maximum error. Results of test cases that did not attain convergence are omitted.

456 The comparison of the calculated percentiles associated with the error tolerances $\tau=8\%$ and $\tau=2\%$, shows that the smallest error tolerance renders the best reproduction of the FSM percentiles. The maximum relative errors in both the 10th- and 90th-percentiles are associated with $\sigma_Y^2=0.1$ and $\tau=8\%$. This is likely related to the small number of basis functions returned by the greedy algorithm in these two cases ($N_{BF} = 3$ for $L_x/\lambda = 3$ and $N_{BF} = 2$ for $L_x/\lambda = 1.5$). We note that this effect is not visible for $\tau=2\%$, where the errors on the percentiles are of the same order of magnitude for all tested cases. Similarly to what observed for the errors on the head variance (Section 5.3), the magnitude of the relative errors on the percentiles are significantly smaller than the error tolerances τ at most locations in the domain. Finally, Figs. 8 and 9 present a comparison between the complete empirical pdfs of the FSM and ROMC head realizations at five selected points in the system. Results are illustrated for two test cases ($L_x/\lambda=3$, $\sigma_Y^2=0.1$ or 1.0) and error tolerances $\tau=8\%$, 2%. The small differences between the pdfs, which have also been detected in the analysis of the head variance and percentiles, do not appear to

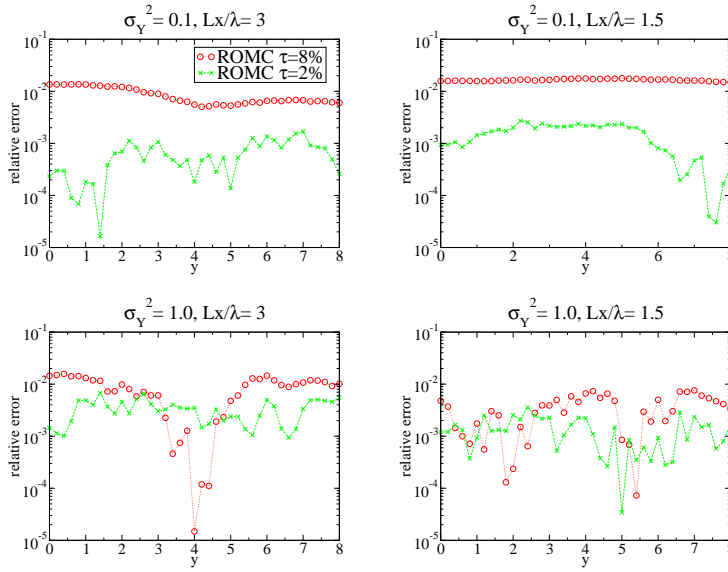


Fig. 6 Relative errors on the 10^{th} -percentile, q_{10} , of hydraulic head along the cross-section normal to the mean flow direction and passing through the domain centre.

472 be significant when we consider the complete range of the hydraulic heads
 473 $[0 \leq h \leq 10]$, resulting from the collection of MC realizations.

474 Results of comparable quality are obtained also for the remaining test cases
 475 (not shown).

476 6 Conclusions

477 Our work leads to the following major conclusions.

478 – The greedy algorithm is a suitable procedure to construct a reduced order
 479 model for the solution of steady-state groundwater flow in the presence of
 480 randomly distributed (Gaussian) log-transmissivities characterized by rel-
 481 atively low variance and highly persistent spatial distribution (i.e., large
 482 correlation length scales relative to the size of the domain). Our examples
 483 show that under these conditions the algorithm reduces the original FSM
 484 of dimension $n=3371$ to a RM of dimension $N_{BF} < 50$ maintaining a high
 485 level of accuracy on each realization of hydraulic heads (see Fig. 2, for the
 486 test cases with $\sigma_Y^2 < 0.5$ and $L_x/\lambda < 3$, with $\tau=2\%$). In these cases, the
 487 procedure requires only a few FSM runs and is markedly advantageous
 488 with respect to the computational cost associated with the classical MC
 489 scheme (10^4 FSM runs in our case). An efficient and accurate reduction for

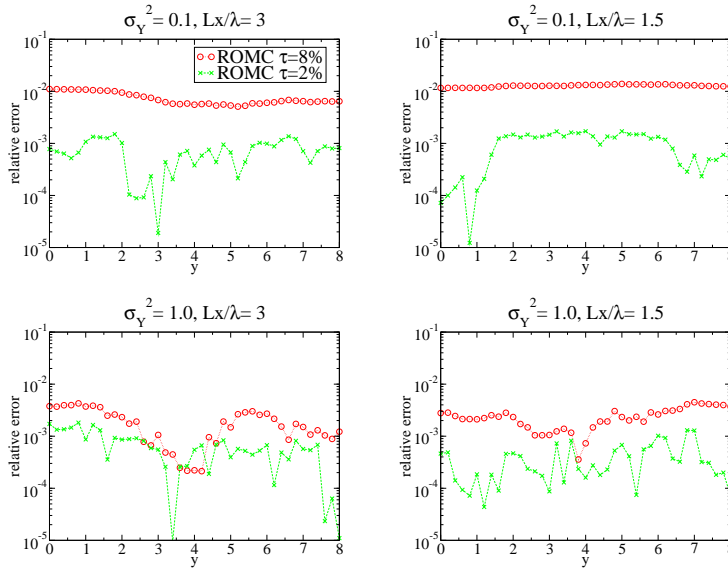


Fig. 7 Relative errors on the 90th-percentile, q_{90} , of hydraulic heads along the cross-section normal to the mean flow direction and passing through the domain center.

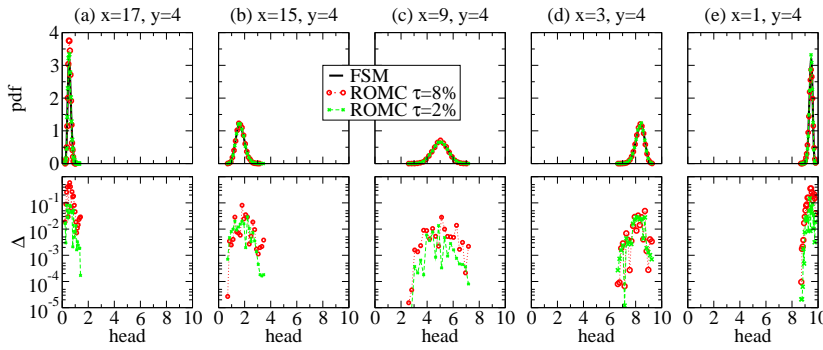


Fig. 8 Comparison between the empirical pdfs of the FSM and ROMC head realizations at the five control points depicted in Fig. 1. Results for $L_x/\lambda=3$ and $\sigma_Y^2=0.1$ and error tolerances $\tau=8\%$, 2% . The lower panels show the absolute differences (Δ) between the ROMC and the FSM results.

490 the configurations characterized by higher variances and smaller correlation
 491 lengths requires setting increased values of the error tolerance τ , even
 492 though this compromises the accuracy on the reproduction of the head
 493 realizations and the empirical head distributions (Figs. 3, 4, and 5).

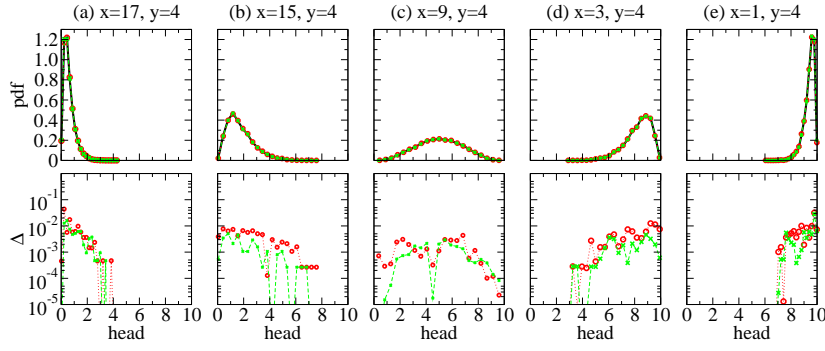


Fig. 9 Comparison between the complete empirical pdfs of the FSM and ROMC head realizations at the five control points depicted in Fig. 1. Results for $L_x/\lambda=3$ and $\sigma_Y^2=1.0$ and error tolerances $\tau=8\%$, 2% . The lower panels show the absolute differences (Δ) between the ROMC and the FSM results.

- 494 – The rate of convergence of the largest error on the head realizations can be
 495 approximated as a power law function of the number of iterations of the
 496 greedy algorithm (Fig. 2, Table 1). This relationship between errors and
 497 number of iterations can be considered as an “a priori” criterion to establish
 498 the number of iterations of the greedy algorithm that are required to reach
 499 the desired error tolerance. Note that, since the implementation of the
 500 greedy algorithm with the residual-based estimation of the error may lead
 501 to a selection of snapshots that do not minimize the discrepancy between
 502 the FSM and ROMC, the convergence rate of the algorithm that employs
 503 residual based error estimations may be slower than the one presented here.
- 504 – The collection of hydraulic head realizations computed with the reduced
 505 order model is associated with an empirical probability distribution that
 506 well approximates the FSM-based sample distribution. We demonstrate
 507 this by showing comparisons of the spatial variance of heads (Figs. 3, 4,
 508 and 5), the spatial distribution of head percentiles along selected domain
 509 cross sections (Figs. 6 and 7) and the entire empirical pdf at selected grid
 510 nodes (Fig. 8 and 9) calculated through the FSM and RM set of real-
 511 izations. As expected, the error on the ensemble statistics decreases with
 512 decreasing error tolerance in the greedy algorithm. It can be noted that,
 513 once the error tolerance τ is assigned, the accuracy of the estimation of
 514 the head statistics is not significantly deteriorated by changes in the geo-
 515 statistical parameters that describe the random spatial distribution of the
 516 log-transmissivity.

517 **Acknowledgements** Funding from MIUR (Italian Ministry of Education, Universities and
518 Research - PRIN2010-11; project “Innovative methods for water resources under hydro-
519 climatic uncertainty scenarios”), from EU FP7 (project CLIMB “Climate Induced Changes
520 on the Hydrology of Mediterranean Basins - Reducing Uncertainty and Quantifying Risk”)
521 and from the Fondazione CaRiPaRO (project “Nonlinear Partial Differential Equations:
522 models, analysis, and control-theoretic problems”) is acknowledged.

References

1. G. Dagan. *Flow and Transport in Porous Formations*. Springer, New York, 1989.
2. D. Zhang. *Stochastic Methods for Flow in Porous Media: Copying With Uncertainties*. Academic Press, San Diego, CA, 2002.
3. A. Yustres, L. Asensio, J. Alonso, and V. Navarro. A review of Markov Chain Monte Carlo and information theory tools for inverse problems in subsurface flow. *Comput. Geosci.*, 16(1):1–20, 2012. doi: 10.1007/s10596-011-9249-z.
4. H. Moradkhani, C. M. DeChant, and S. Sorooshian. Evolution of ensemble data assimilation for uncertainty quantification using the particle filter-Markov chain Monte Carlo method. *Water Resour. Res.*, 48(12):W12520, 2012. doi: 10.1029/2012WR012144.
5. A. Guadagnini and S. P. Neuman. Nonlocal and localized analyses of conditional mean steady state flow in bounded, randomly nonuniform domains: 1. Theory and computational approach. *Water Resour. Res.*, 35(10):2999–3018, 1999. doi: 10.1029/1999WR900160.
6. C. L. Winter, D. M. Tartakovsky, and A. Guadagnini. Moment differential equations for flow in highly heterogeneous porous media. *Surv. Geophys.*, 24(1):81–106, 2003. doi: 10.1023/A:1022277418570.
7. M. Panzeri, M. Riva, A. Guadagnini, and S. P. Neuman. Data assimilation and parameter estimation via ensemble Kalman filter coupled with stochastic moment equations of transient groundwater flow. *Water Resour. Res.*, 49, 2013. doi: 10.1002/wrcr.20113.
8. X. Sanchez-Vila, D. Fernandez-Garcia, and Guadagnini A. Conditional probability density functions of concentrations for mixing-controlled reactive transport in heterogeneous aquifers. *Math. Geosci.*, 41:323–351, 2009. doi: 10.1007/s11004-008-9204-2.
9. D. M. Tartakovsky, M. Dentz, and P. C. Lichtner. Probability density functions for advective-reactive transport in porous media with uncertain reaction rates. *Water Resour. Res.*, 45:W07414, 2009. doi: 10.1029/2008WR007383.

10. M. Dentz and D. M. Tartakovsky. Probability density functions for passive scalars dispersed in random velocity fields. *Geophys. Res. Lett.*, 45:L24406, 2010. doi: 10.1029/2010GL045748.
11. D. Venturi, D. M. Tartakovsky, A. M. Tartakovsky, and G. E. Karniadakis. Exact pdf equations and closure approximations for advective-reactive transport. *J. Comp. Phys.*, 243:323–343, 2013. doi: 10.1016/j.jcp.2013.03.001.
12. F. Ballio and A. Guadagnini. Convergence assessment of numerical Monte Carlo simulations in groundwater hydrology. *Water Resour. Res.*, 40:W04603, 2004. doi: 10.1029/2003WR002876.
13. D. Pasetto, A. Guadagnini, and M. Putti. POD-based Monte Carlo approach for the solution of regional scale groundwater flow driven by randomly distributed recharge. *Adv. Water Resources*, 34(11):1450–1463, 2011. doi: 10.1016/j.advwatres.2011.07.003.
14. D. Zhang and Z. Lu. An efficient, high-order perturbation approach for flow in random porous media via Karhunen-Loève and polynomial expansions. *J. Comp. Phys.*, 194(2):773 – 794, 2004. doi: 10.1016/j.jcp.2003.09.015.
15. S. Poles and A. Lovison. A polynomial chaos approach to robust multiobjective optimization. In Deb, K., et al., editor, *Hybrid and Robust Approaches to Multiobjective Optimization*, number 09041 in Dagstuhl Seminar Proceedings. Schloss Dagstuhl - Leibniz-Zentrum fuer Informatik, Germany, Dagstuhl, Germany, 2009.
16. S. Oladyshkin, H. Class, R. Helmig, and W. Nowak. An integrative approach to robust design and probabilistic risk assessment for CO2 storage in geological formations. *Comput. Geosci.*, 15(3):565–577, 2011. doi: 10.1007/s10596-011-9224-8.
17. L. Formaggia, A. Guadagnini, I. Imperiali, V. Lever, G. Porta, M. Riva, A. Scotti, and L. Tamellini. Global sensitivity analysis through polynomial chaos expansion of a basin-scale geochemical compaction model. *Comput. Geosci.*, 17:25–42, 2013. doi: 10.1007/s10596-012-9311-5.
18. H. Li and D. Zhang. Probabilistic collocation method for flow in porous media: Comparisons with other stochastic methods. *Water Resour. Res.*, 43:W09409, 2007. doi: 10.1029/2006WR005673.
19. K. Kunisch and S. Volkwein. Galerkin proper orthogonal decomposition methods for a general equation in fluid dynamics. *SIAM J. Num. Anal.*, 40:492–515, 2002. doi: 10.1137/S0036142900382612.
20. A. J. Siade, M. Putti, and W. W.-G. Yeh. Snapshot selection for groundwater model reduction using proper orthogonal decomposition. *Water Resour. Res.*, 46:W08539, 2010. doi: 10.1029/2009WR008792.
21. M. A. Grepl and A. T. Patera. A posteriori error bounds for reduced-basis approximations of parametrized parabolic partial differential equations. *ESAIM-Math. Model. Num.*, 39(1):157–181, 2005. doi: 10.1051/m2an:2005006.
22. A. Quarteroni, G. Rozza, and A. Manzoni. Certified reduced basis approximation for parametrized partial differential equations and applications.

-
- Math. Indust.*, 1(1):1–49, 2011. doi: 10.1186/2190-5983-1-3.
23. A. J. Siade, M. Putti, and W. W.-G. Yeh. Reduced order parameter estimation using quasilinearization and quadratic programming. *Water Resour. Res.*, 48:W06502, 2012. doi: 10.1029/2011WR011471.
 24. M. P. Kaleta, R. G. Hanea, A. W. Heemink, and J-D. Jansen. Model-reduced gradient-based history matching. *Comput. Geosci.*, 15(1):135–153, 2011. doi: 10.1007/s10596-010-9203-5.
 25. J. F. M. van Doren, R. Markovinović, and J-D. Jansen. Reduced-order optimal control of water flooding using proper orthogonal decomposition. *Comput. Geosci.*, 10(1):137–158, 2006. doi: 10.1007/s10596-005-9014-2.
 26. D. Pasetto, M. Putti, and W. W-G. Yeh. A reduced order model for groundwater flow equation with random hydraulic conductivity: application to Monte Carlo methods. *Water Resour. Res.*, 49:1–14, 2013. doi: 10.1002/wrcr.20136.
 27. F. Müller, P. Jenny, and D. W. Meyer. Multilevel Monte Carlo for two phase flow and Buckley-Leverett transport in random heterogeneous porous media. *J. Comp. Phys.*, 2013. doi: 10.1016/j.jcp.2013.03.023.
 28. C. Lieberman, K. Willcox, and O. Ghattas. Parameter and state model reduction for large-scale statistical inverse problems. *SIAM J. Sci. Comput.*, 32(5):2523–2542, 2010. doi: 10.2307/2236101.
 29. A. Bellin and Y. Rubin. HYDRO_GEN: A spatially distributed random field generator for correlated properties. *Stoch. Hydrol. Hydraul.*, 10(4): 253–278, 1996. doi: 10.1007/BF01581869.